

**IDETC2016-59386**

## DESIGN AND ANALYSIS OF A MINIATURE MODULAR INCHWORM ROBOT

**Wael Saab**

Robotics and Mechatronics  
Laboratory  
Virginia Tech  
Blacksburg, VA 24061

**Anil Kumar**

Robotics and Mechatronics  
Laboratory  
Virginia Tech  
Blacksburg, VA 24061

**Pinhas Ben-Tzvi**

Robotics and Mechatronics Laboratory  
Virginia Tech  
Blacksburg, VA 24061  
[bentzvi@vt.edu](mailto:bentzvi@vt.edu)

### ABSTRACT

This paper presents the design and analysis of a bio-inspired miniature modular Inchworm robot. Inchworm robots play crucial roles in surveillance, exploration and search and rescue operations where maneuvering in confined spaces is required. Rectilinear gaits have been demonstrated with favorable results in terms of stability and small size due to the absence of wheels and tracks; however, exhibit slow speeds. The proposed mechanism utilizes undulatory rectilinear gait motion through linear expansion/contraction of modules and anisotropic friction skin to produce pure linear motion. The use of anisotropic friction skin results in a simple, low cost, miniature mechanical structure. Friction analysis of the anisotropic material is performed and the system is modeled to derive its equations of motion. Modeling and simulation results are validated through experiments performed with an integrated prototype. Results indicate that the robot can achieve an average forward velocity of 11 mm/s on various surfaces.

### 1 INTRODUCTION

Animals have evolved over millions of years to adapt to their natural habitat. They utilize a wide range of locomotion mechanisms to traverse terrain ranging from legged locomotion using limbs and joints to inchworm-like locomotion that involves repeated body expansions and contractions. These animals have inspired engineers to develop “bio-inspired” robots. Legged robots have been developed in literature; however, they require a large number of actuators and potentially-complicated body structures to mimic locomotion patterns of animal counterparts [1-3]. Since it’s difficult to apply such mechanisms for small scale applications, inchworm like locomotion has been investigated for centimeter-scale robotic applications [4-6].

In both legged and inchworm like systems, bi-directional adhesion properties can be used to provide enhanced

locomotion. For example, Geckos can climb up inclined surfaces using directional foot pads [7]. Gastropods generate wave undulations using muscles within its body to create differences in reactive and frictional forces to move forward [8]. It has also been observed that slanted claws of insects also prevent backward slipping [9]. These animals have motivated researchers to integrate bi-directional adhesion materials into in robotic systems [10-12].

Inchworms locomote using vertical wave undulation that involves lifting its front body and displacing it with respect to its remaining stationary body [13]. Rectilinear undulatory gait motions are appealing to robotic applications since locomotion can be achieved without the need for expensive treads or wheels that take up additional space and limit the compactness of the robot’s design. This gait also enables robots to perform motion on wide variety of terrains, as the robot can adjust its shape to fit the terrain contour. However, because of the wasted time and energy spent on lifting and lowering the modules normal to the robots trajectory, this motion can result in low forward velocities and limited range. Additionally, the extra required energy necessitates a larger chassis for storing additional sources of energy and makes these robots less suitable for operation in confined spaces [14].

To overcome these problems, we propose a bio-inspired miniature modular inchworm robot (MMIR) that utilizes rectilinear expansion and contraction locomotion and an anisotropic-friction skin to produce forward and steering motions. The aim of this research is to develop a small scale, low cost robot and investigate its performance through modeling, simulation and experimentation on various types of terrain.

The structure of this paper is as follows. Section 2 provides an overview of existing robots in literature. Section 3 presents the design and prototype integration of the MMIR. Section 4 shows a friction analysis of the anisotropic-friction skin. The

equations of motion are derived in Section 5 and simulated in Section 6. Section 7 experimentally validates the simulation results. Closing remarks and future work are discussed in Section 8.

## 2 RELATED WORK

This section reviews the state of the art of robots utilizing undulatory gaits and bi-directional adhesion properties to produce locomotion.

The Slim Slime Robot [15] is an active-cord mechanism designed with 3 serially-connected modules actuated by bellows that are capable of shrink, stretch, and locking. This enabled 3-dimensional locomotion. The robot demonstrated a maximum forward locomotion 60 mm/s by sliding only one module forward at a time while the combined friction forces of the remain two modules prevented backwards slipping. The robot measured 128 mm in diameter with a total contracted length of 730 mm.

Similarly, the Active Cord Mechanism – Slime model 1 [16] was designed with six ratcheted wheels surrounding the body and a bending and expanding, three degree of freedom (3 DOF) joint unit to allow both inchworm-like and angleworm-like motion. The inchworm-like motion demonstrated a slow gait but was capable of traversing bumpy or uneven ground. In contrast, the angleworm-like motion used little energy for fast motion on flat ground, but was ineffective on uneven ground. A single joint unit of the robot had a length of between 168 and 268 mm with an 80 mm diameter.

The Maryland Snake Inspired Robot [14] consisted of 3-DOF joint modules each with 2 revolute joints, that rotated in orthogonal planes with respect to one another, and a prismatic joint. Joint modules were stacked serially with 90 degree offsets and a 1-DOF friction-anchor module was placed at either end of the robot to grip the environment. To achieve either turning or forward motion the joint modules would perform either rotation or linear expansion respectively. The robot had a compressed length of 1003 mm with a cross-section of 70x70 mm and can move forward at a speed of 167 mm/s.

Chen et al. proposed a Planar Inchworm Robot [17] designed for applications in narrow and confined spaces such as pipes and conduits. The robot consisted of 1-DOF modules that could function as either grippers that grasp the terrain to increase friction or extensors that deform in the direction of the robot's motion. Further work on the PIR resulted in the development of the Planar Walker [18]. It contained linear cylinders and four revolute joints to form a closed-loop, eight-bar mechanism. Four pneumatic suction modules were mounted below each revolute joint to grip the terrain, holding the robot to its surface. While it mimicked snake or inchworm-like creeping motions, its unique mechanical design also allowed for swift changes in the direction of travel.

An earthworm-like robot created by Kim et al [4] used a shape memory alloy actuator between two segments to create relative translation between two bodies. Each body had a passive needle that grips onto a soft environment to prevent backward slipping. The robot measured 50 mm in length and

9.5 mm in diameter and can move forward at a speed of 0.16 mm/s.

An earthworm robot that consisted of eight soft body segments was investigated in [19, 20]. It produced forward linear motion by expanding and contracting its soft bodies by pulling cables. The robot generated forward locomotion by keeping a larger number of body segments stationary while sliding the remaining segments forward. This generated an anchoring friction that prevented backwards slipping. The maximum average speed achieved was 10 mm/s.

Climbing machines that utilize pneumatic actuators and cylindrical, metallic brushes, with a slightly larger diameter than a pipe bore, have demonstrated an effective means of locomotion for traversing pipe and sewer systems [21]. This concept was further investigated on an Active Scope Camera robot in [22, 23]. The robot consisted of a long cable covered with cilia in the form custom designed thin wires oriented at a specific angle to provide unidirectional anchorage with respect to a flat floor. It utilized vibration drive and an inchworm drive (pneumatic cylinder) combined with the cilia friction properties to propel the robot forward. The test robot used had a length of 800 mm and a diameter of 24 mm. Depending on the terrain, the speed varied from 20 to 100 mm/s.

## 3 DESIGN CONCEPT

The concept of the MMIR was inspired by the biological anatomy of an Inchworm. Fig. 1 depicts the computer aided design (CAD) model of the assembled MMIR. Modules, representing an inchworm's front and rear body, translate relative to one another along the robots length to produce relative motion. Located on both the top and bottom sides of each module is an anisotropic friction skin. This friction skin is an artificial, commercially available fabric with compliant,

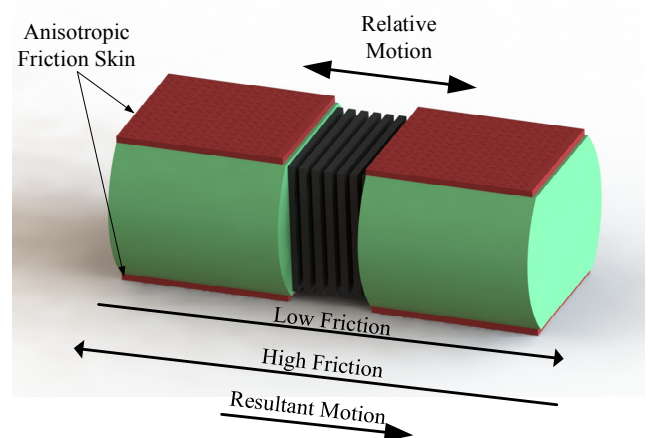


**Figure 1. CAD model of the assembled MMIR**

sharp bristles oriented at an inclined angle with respect to its flat surface. The skin exhibits low friction along the direction the bristles are oriented since their compliance results in a

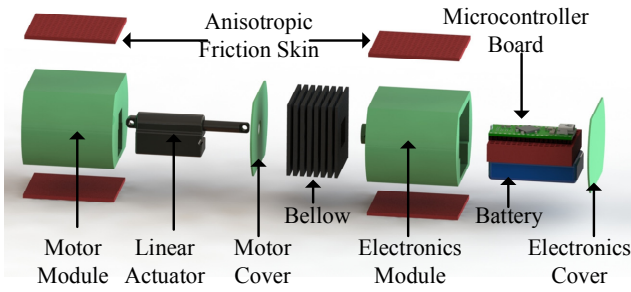


**Figure 2. Exploded view of MMIR**

smooth flat surface. In the opposing direction, the bristles oppose motion by engaging/meshing with micro-sized surface irregularities. Modules have curved side profiles and have the friction skin oriented in the same direction to ensure the MMIR continuously moves forward if flipped over.

Fig. 2 shows an exploded view of the MMIR. The robot consists of a motor and electronics module. The motor module contains a micro sized linear actuator capable producing a maximum force of 35 N, and travel at a speed of 25 mm/s with a 20 mm stroke length. The linear actuator has an inbuilt resistive potentiometer which acts as position sensor for the actuator shaft. The electronics module contains a 450 mAh, 7.4 V battery and mini bread board on to which an ARM Cortex M4 microcontroller and other mounted electronics. The microcontroller is programmed to generate sinusoidal force for periodic expansion and contraction between the two modules. The electronics module is rigidly connected to the shaft of the linear actuator. Covers and a flexible custom made bellow provide a dust proof enclosure to protect the internal components of each module from the external environment; thus, making the robot applicable for harsh conditions. The bellow also prevents any object from getting stuck between the two blocks during contraction that can cause jamming.

Fig. 3 shows the integrated prototype of the MMIR. Over all dimensions of the robot measure 10 cm in length with a cross sectional area equivalent to 44x44mm. Total weight of the assembled prototype was 190g.

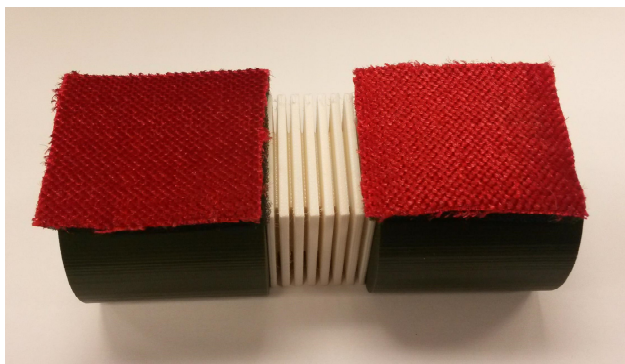


**Figure 3. Integrated prototype of MMIR.**

#### 4 FRICTION ANALYSIS

Differential friction provides the sole driving force for the operation of the MMIR. The anisotropic friction skin offers low friction in forward slide motion but much higher friction in the opposing direction. Thus, when the linear actuator between the two modules expands and contracts, only one module will slide forward while the other acts as an anchored base due to high friction.

The friction coefficients were experimentally determined by measuring the critical plane angle of inclination that caused a black mass covered with the anisotropic friction material to start slipping due to its weight. The maximum and minimum friction coefficients between the anisotropic friction skin and different materials are summarized in Table 1.  $\theta$  is the critical inclination angle (degrees) and  $\mu$  is the coefficient of friction. The subscripts 'L' and 'H' represent the smooth (with low friction) and rough (with high friction) direction of the anisotropic friction skin used on MMIR.

**Table 1. Friction coefficient of different materials**

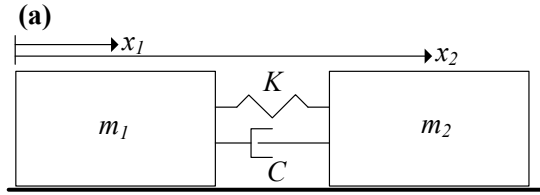
Material	$\theta_L^\circ$	$\mu_L$	$\theta_H^\circ$	$\mu_H$
Cast Iron	16	0.287	22	0.404
Anodized Aluminum	23	0.4245	23	0.4245
Carpet	29	0.5545	76	4.01
Polished Wood	36	0.7265	41	0.8693
Concrete Bar	44	0.9657	52	1.2799
Paper	22	0.404	43	0.9325
Floor Tiles	23	0.4245	38	0.7813

#### 5 KINEMATIC MODEL

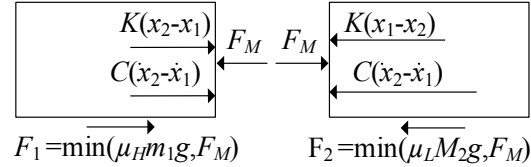
To derive the equations of motion of the MMIR, the system was modelled as two bodies with mass  $m_1$  and  $m_2$  connected with a spring and a damper with coefficients  $K$  and  $C$  respectively (with reference to Fig. 4 (a)). The spring constant is a result of elastic nature of the linear actuator where damping is the resultant of electromagnetic damping of the motor in the form of back EMF. Figs. 4 (b) and (c) show the free body diagram of the MMIR during the expansion and contraction stroke respectively.

$F_M$  represents the force applied by the motor,  $x_1$  and  $x_2$  are positions of the bodies. It is assumed that the anisotropic friction skin is attached to the MMIR such that there is minimum friction in forward direction and maximum friction backwards. The motion of the MMIR can be decomposed into two strokes: the expansion stroke and the contraction stroke. Equation (1) and (2) describe the equation of motion for the two blocks as shown in Fig. 4. The upper sign apply in case of expansion stroke whereas the lower sign describes the contraction stroke.

$$K = \begin{cases} 0; & \text{abs}(x_2 - x_1) < S \\ \infty; & \text{abs}(x_2 - x_1) \geq S \end{cases} \quad (3)$$



(b) — Expansion Stroke



(c) Contraction Stroke

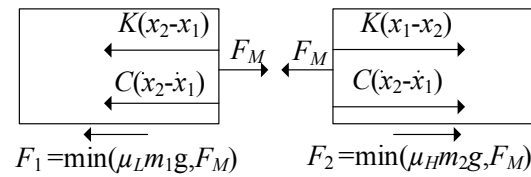


**Figure 4. (a) Kinematic model of MMIR. Free body diagrams of (b) expansion and (c) contraction**

$$m_1 \ddot{x}_1 = \mp F_M \pm K(x_2 - x_1) \pm C(\dot{x}_2 - \dot{x}_1) \pm F_1 \quad (1)$$

$$m_2 \ddot{x}_2 = \pm F_M \mp K(x_1 - x_2) \mp C(\dot{x}_1 - \dot{x}_2) \mp F_2 \quad (2)$$

Through simple analysis of the free body diagram, conditions may be derived to ensure successful forward motion of the robot given by  $\mu_H m_1 g > F_M > \mu_L m_2 g$  and  $\mu_L m_1 g < F_M < \mu_H m_2 g$  for expansion and contraction strokes, respectively. It is intuitive to observe that a large difference in the masses of the two blocks will not satisfy the above conditions and could result in undesirable backward slippage motion. As  $\mu_H \geq \mu_L$ , for maximum efficiency to produce forward motion without backward slippage, it is ideal to have identical masses (i.e.  $m_1 = m_2$ ). Originally, the motor module was lighter than the module that houses the electronics. To make both modules of the same weight, motor module cavity was filled with miniature lead weights resulting in final prototype total mass of 190g.

## 6 SIMULATION

To assess the performance of MMIR, a simulation study was conducted. For simulation, the actuator force was modelled with sinusoidal function with a magnitude of 35N (rated actuator force). To model the physical displacement limitation due to stroke length of the actuator, the spring coefficient was modeled as step function given in equation (3).

where  $S$  is the maximum stroke length of the motor and  $(x_2 - x_1)$  is the motor stroke. Using this method, the infinite value of  $K$  occur at minimum and maximum values of relative displacement between two modules; thus, maintaining the relative displacement within physical limitations of the system. Table 2 shows the simulation parameters used in the study:

**Table 2. Simulation Parameters**

Parameter	Value
$m_1, m_2$	0.095 kg
$\mu_H$	0.86
$\mu_L$	0.72
$C$	0.001 Ns/m
$A$	3
$S$	50
$\phi$	0.5

ODE45 differential equation solver in MATLAB™ was used to solve the equations of motion given in Eq.(1)-(2) and simulate locomotion on a wooden surface. Fig. 5 shows the simulation results including position and velocity plots of the MMIR modules as a function of time. As observed from the figure, the average forward moving speed of the modules is calculated to be approximately 10 mm/s.

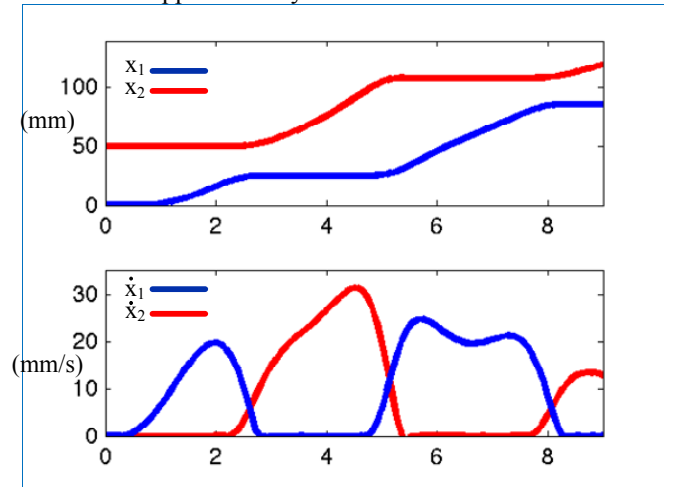


**Figure 5. Simulation result: displacement (top) and velocity (bottom) plots of the two modules.**

## 7 EXPERIMENTAL RESULTS

To assess the performance of MMIR, two experiments were conducted. In the first experiment, the forward velocity of the robot was measured on five surfaces which were analyzed in Section 4. Table 3 shows the average speed of MMIR achieved on different surfaces. The MMIR failed to produce any forward motion on anodized aluminum due to the same high and low friction coefficients measured in Section 4. On the remaining

surfaces, the robot successfully moves forward with no slipping. Variations in forward velocity are due to the various friction coefficients of each surface. In addition, the forward velocity of the robot matched the average forward velocity computed in simulations for a wooden surface. During experiments, the stride frequency was set to 1 Hz and the stride length was set to 20 mm (limited by the linear actuator).

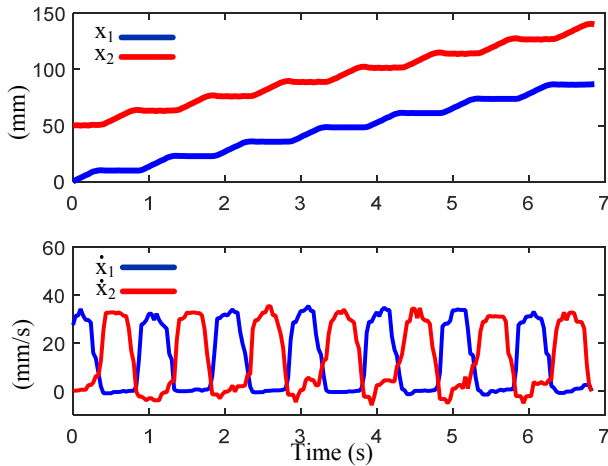


**Figure 6. Experimental results (floor tiles): displacement (top) and velocity (bottom) plots of the two modules on floor tiles.**

Fig. 6 shows instantaneous position and velocity of MMIR modules measured using optical tracking. A calibrated camera was used to track positions of the two markers placed on the center of each of the two modules. The velocity estimates were obtained by taking time derivative of the measured position. During experiments, slight back slippage (in the form of -ve velocity) was observed in the second modules due to slight mismatch in the weights of the two modules. The position and velocity profiles matched closely with the simulation results.

**Table 3. Measured forward velocity experimental results**

Material	Velocity (mm/s)
Anodized Aluminum	0 (slippage)
Carpet	12.74
Polished Wood	11
Paper	11.9
Floor Tiles	12.38

In a separate experiment, turning capabilities of the robot was investigated. Modules were physically oriented with a printed connector unit at a  $5^\circ$  angle with respect to one another. It was hypothesized that the left and right curvature turns may be possible due to a moment generated from the anisotropic friction skin unidirectional angled frictional force when the

robot performs the identical undulatory gait like motion using a sinusoidal linear expansion and contraction.

This hypothesis was validated as observed in Fig. 7, which depicts visual tracking of the modified MMIR performing a right curvature turn. The top layer of the friction skin was removed to identify corners using image processing. Optical tracking methods conclude that the robot is capable of performing a 64.5 cm radius curvature turn when modules are aligned at a  $5^\circ$  angle. This steering capability of the MMIR will be exploited in future work with better performance expected with larger tilt angles between the modules.



**Figure 7. Steering of MMIR on wood.**

## 8 CONCLUSION AND FUTURE WORK

A bio-inspired inchworm robot is presented in this paper that utilizes undulatory rectilinear gait motion through linear expansion/contraction of modules and anisotropic friction skin, to produce pure linear motion. The use of anisotropic friction skin results in a simple, low cost, miniature mechanical structure. Results demonstrate the robot is capable of forward locomotion on various materials that exhibit bi-directional adhesion properties at an average speed of approximately 11 mm/s.

In terms of ongoing research, MMIR Generation 2 (G2), shown in Fig. 8, is currently being developed to further increase locomotion capabilities and provide a wide range of sensing technologies while keeping the overall dimensions of the robot 10 cm in length with a cross sectional area equivalent to 44x44mm.

The major improvement in MMIR-G2 is the addition of a slider crank four bar mechanism that will provide high speed relative translation between modules to enable a greater forward velocity in comparison to a linear actuator. In addition, a servo motor will connect the slider to the electronics module to provide relative rotation and enable left and right steering. The robot will be supplemented an custom PCB integrated with sensors like IMU, a wireless camera Xbee® WiFi™ module to provide orientation information, live video streaming, and teleoperation capabilities using wireless peer-to-peer connectivity, which is essential for applications such as surveillance, monitoring and mapping of hazardous environments.

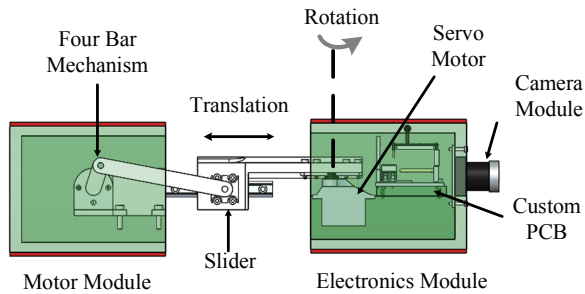


**Figure 8. Miniature Modular Inchworm Robot G2.**

## REFERENCES

- [1] Birkmeyer, P., Peterson, K., and Fearing, R. S., 2009, "Dash: A Dynamic 16g Hexapedal Robot," *Proc. IEEE/RSJ International Conference on Intelligent Robots and Systems*, IEEE, pp. 2683-2689.
- [2] Kim, S., Clark, J. E., and Cutkosky, M. R., 2006, "Isprawl: Design and Tuning for High-Speed Autonomous Open-Loop Running," *The International Journal of Robotics Research*, 25(9), pp. 903-912.
- [3] Saranlı, U., Buehler, M., and Koditschek, D. E., 2001, "Rhex: A Simple and Highly Mobile Hexapod Robot," *The International Journal of Robotics Research*, 20(7), pp. 616-631.
- [4] Kim, B., Lee, M. G., Lee, Y. P., Kim, Y., and Lee, G., 2006, "An Earthworm-Like Micro Robot Using Shape Memory Alloy Actuator," *Sensors and Actuators A: Physical*, 125(2), pp. 429-437.
- [5] Koh, J.-S., and Cho, K.-J., 2009, "Omegabot: Biomimetic Inchworm Robot Using Sma Coil Actuator and Smart Composite Microstructures (Scm)," *Proc. IEEE International Conference on Robotics and Biomimetics* IEEE, pp. 1154-1159.
- [6] Lim, J., Park, H., An, J., Hong, Y.-S., Kim, B., and Yi, B.-J., 2008, "One Pneumatic Line Based Inchworm-Like Micro Robot for Half-Inch Pipe Inspection," *Mechatronics*, 18(7), pp. 315-322.
- [7] Autumn, K., and Peattie, A. M., 2002, "Mechanisms of Adhesion in Geckos," *Integrative and Comparative Biology*, 42(6), pp. 1081-1090.
- [8] Denny, M. W., 1981, "A Quantitative Model for the Adhesive Locomotion of the Terrestrial Slug, *Ariolimax Columbianus*," *Journal of experimental Biology*, 91(1), pp. 195-217.
- [9] Stork, N., 1980, "Experimental Analysis of Adhesion of *Chrysolina Polita* (Chrysomelidae: Coleoptera) on a Variety of Surfaces," *The Journal of Experimental Biology*, 88(1), pp. 91-108.
- [10] Spenko, M., Haynes, G. C., Sanders, J., Cutkosky, M. R., Rizzi, A. A., Full, R. J., and Koditschek, D. E., 2008, "Biologically Inspired Climbing with a Hexapedal Robot," *Departmental Papers (ESE)*, p. 397.
- [11] Kim, S., Asbeck, A. T., Cutkosky, M. R., and Provancher, W. R., 2005, "Spinybotii: Climbing Hard Walls with Compliant Microspines," *Proc. 12th International Conference on Advanced Robotics*, IEEE, pp. 601-606.
- [12] Kim, S., Spenko, M., Trujillo, S., Heyneman, B., Mattoli, V., and Cutkosky, M. R., 2007, "Whole Body Adhesion: Hierarchical, Directional and Distributed Control of Adhesive Forces for a Climbing Robot," *Proc. IEEE International Conference on Robotics and Automation*, IEEE, pp. 1268-1273.
- [13] Transth, A. A., Pettersen, K. Y., and Liljebäck, P., 2009, "A Survey on Snake Robot Modeling and Locomotion," *Robotica*, 27(07), pp. 999-1015.
- [14] Hopkins, J. K., and Gupta, S. K., 2014, "Design and Modeling of a New Drive System and Exaggerated Rectilinear-Gait for a Snake-Inspired Robot," *Journal of Mechanisms and Robotics*, 6(2), p. 021001.
- [15] Ohno, H., and Hirose, S., 2001, "Design of Slim Slime Robot and Its Gait of Locomotion," *Proc. IEEE/RSJ International Conference on Intelligent Robots and Systems*, IEEE, pp. 707-715.
- [16] Sugita, S., Ogami, K., Michele, G., Hirose, S., and Takita, K., 2008, "A Study on the Mechanism and Locomotion Strategy for New Snake-Like Robot Active Cord Mechanism—Slime Model 1 Acm-S1," *Journal of Robotics and Mechatronics*, 20(2), pp. 302-309.
- [17] Chen, I., Yeo, S. H., and Gao, Y., 2001, "Locomotive Gait Generation for Inchworm-Like Robots Using Finite State Approach," *Robotica*, 19(05), pp. 535-542.
- [18] Yeo, S. H., Chen, I.-M., Senanayake, R., and Wong, P. S., "Design and Development of a Planar Inchworm Robot," *Proc. Proceedings of the 17th IAARC International Symposium on Automation and Robotics in Construction, Taipei, Taiwan*.
- [19] Fang, H., Wang, C., Li, S., Wang, K. W., and Xu, J., 2015, "A Comprehensive Study on the Locomotion Characteristics of a Metameric Earthworm-Like Robot," *Multibody Syst Dyn*, 35(2), pp. 153-177.
- [20] Fang, H., Li, S., Wang, K. W., and Xu, J., 2015, "A Comprehensive Study on the Locomotion Characteristics of a Metameric Earthworm-Like Robot," *Multibody Syst Dyn*, 34(4), pp. 391-413.
- [21] Appleton, E., and Stutchbury, N. W., 2000, "Novel Brush Drive Robotic Tractor for Sewer and Water Main Inspection and Maintenance," *Industrial Robot: An International Journal*, 27(5), pp. 370-377.
- [22] Hatazaki, K., Konyo, M., Isaki, K., Tadokoro, S., and Takemura, F., 2007, "Active Scope Camera for Urban Search and Rescue," *Proc. IEEE/RSJ International Conference on Intelligent Robots and Systems*, IEEE, pp. 2596-2602.
- [23] Ishikura, M., Wakana, K., Takeuchi, E., Konyo, M., and Tadokoro, S., 2011, "Running Performance Evaluation of Inchworm Drive and Vibration Drive for Active Scope Camera," *Proc. IEEE/ASME International Conference on Advanced Intelligent Mechatronics* IEEE, pp. 599-604.